

Low-temperature “Depletion” of Superfluid Density

Viktor Berger,¹ Nikolay Prokof'ev,¹ and Boris Svistunov¹

¹*Department of Physics, University of Massachusetts, Amherst, MA 01003, USA*

Landau theory of superfluidity associates low-temperature flow of the normal component with the phonon wind. This picture does not apply to superfluids in which Galilean invariance is broken either by disorder, or porous media, or lattice potential, and the phonon wind is no longer responsible for depletion of the superfluid component. Based on Popov's hydrodynamic action with anharmonic terms, we present a general theory for temperature dependence of the superfluid stiffness at low T , which reproduces Landau result as a special case when several parameters of the hydrodynamic action are fixed by the Galilean invariance. At the technical level, the theory of low-temperature depletion in a d -dimensional quantum superfluid maps onto the problem of finite-size corrections in a $(d + 1)$ -dimensional anisotropic (pseudo-)classical-field system with U(1)-symmetric complex-valued action. We validate our theory with numeric simulations of interacting lattice bosons and the J-current model. In a broader context, our approach reveals universal low-temperature thermodynamics of superfluids.

I. INTRODUCTION

The breathtaking simplicity and asymptotic accuracy (in the low- T limit) of Landau theory of superfluidity [1] comes at a significant price of leaving behind the fundamental concept of superfluid phase [2] and all associated phenomena, such as quantization of the superfluid velocity circulation [3, 4], isolated vortexes and vortex arrays [4, 5], AC Josephson effect [6], etc. Furthermore, one can observe that Landau theory can hardly be used in addressing its own cornerstone question: “What is the general theory (if any) of the low-temperature dependence of the superfluid mass density ρ_s ?”

By general case, we mean systems with continuous translation symmetry being broken either by periodic or disordered external potential. Important examples of such systems include ultracold atoms in optical lattices, supersolids, ^4He in porous media [7], and ^4He films on substrates [8]. The two-fluid picture needs to be seriously revised in all such cases because at $T = 0$ only the superfluid component is flowing while the non-zero normal component is pinned by external potential. Nevertheless, a well-defined long-wave phonon subsystem exists even in this case. The hydrodynamic Hamiltonian describing the phonon subsystem is translation invariant, and one may think that the temperature dependence of depletion can be explained by the phonon wind. In Landau theory, the normal flow and phonon wind are synonymous, thus yielding a straightforward way of calculating the depletion of ρ_s at low temperature: By Galilean invariance, phonon wind in the reference frame moving with the superfluid velocity exactly corresponds to the pure superflow in the reference frame in which the phonon subsystem is at rest. Therefore, the momentum density of the equilibrium phonon wind as a function of its (infinitesimal) velocity immediately yields the normal fraction.

To “quantify” the power and limitations of Landau theory, observe that the derivation of the normal density rests on the Galilean relation between the mass density

flux, \mathbf{j}_m , and momentum density, \mathbf{p} :

$$\mathbf{j}_m = \mathbf{p} \quad (\text{in a Galilean system}). \quad (1)$$

This relation is true no matter whether the system is in the low-temperature regime, where the normal component corresponds to a dilute gas of elementary excitations (phonons), or in a strongly correlated regime of critical fluctuations on approach to the critical temperature. However, only at sufficiently low temperature is Eq. (1) practically useful for obtaining the normal density through a straightforward calculation of the momentum density of non-interacting elementary excitations subject to the Gibbs distribution.

In the absence of continuous translation invariance, the phonon wind will always decay and the genuinely equilibrium superflow regime implies the absence of phonon wind! Therefore, it would be naïve—and, as we will argue, fundamentally wrong—to directly relate the phonon wind momentum as a function of velocity to the depletion of superfluid density. On the other hand, it is reasonable to expect (given that at $T \rightarrow 0$ phonons are the only elementary excitations described by the universal hydrodynamic Hamiltonian) that the temperature dependence of depletion is still universal and even reminiscent of the Landau result, but is controlled by several parameters of the hydrodynamic Hamiltonian that can take rather arbitrary values in a general case. On the qualitative side, the general theory of depletion requires going beyond the harmonic effective Hamiltonian/action. While early treatments of anharmonic terms in the Hamiltonian focused on the kinetics of elementary excitations [9], our statistical treatment also considers higher-order fluctuations of the superfluid field of phase. Reproducing Landau result—originally based on a purely harmonic treatment bootstrapped by the relation (1)—using anharmonic terms in the hydrodynamic Hamiltonian/action is instructive and immediately reveals how special the Galilean invariant systems are. In the general case, even the very notion of temperature induced “depletion” becomes questionable because ρ_s may increase with temperature, i.e. the theory allows depletion to be “negative”!

In this paper, we find that the low-temperature change of the superfluid stiffness (the superfluid density and stiffness, n_s , are simply related by the bare particle mass as $\rho_s = mn_s$), $\Delta n_s(\beta) = n_s(\beta) - n_s(\infty)$, of a d -dimensional superfluid is given by the formula

$$\Delta n_s(\beta) = -\frac{I_d \nu^2 (d+1) - d\gamma n_s - (d+2)\sigma/\varkappa}{d c(c\beta)^{(d+1)}}, \quad (2)$$

$$I_d = \int \frac{d^d q}{(2\pi)^d} \frac{q}{e^q - 1}, \quad (3)$$

$$\nu = \frac{dn_s}{dn}, \quad \gamma = \frac{1}{2} \frac{d^2 n_s}{dn^2}, \quad \sigma = 2 \left. \frac{\partial^2 \mathcal{E}(n, k_0^2)}{\partial (k_0^2)^2} \right|_{k_0=0}, \quad (4)$$

with $\beta = 1/T$ the inverse temperature and n the total number density. All other parameters refer to various ground-state properties: sound velocity, $c = \sqrt{n_s/\varkappa}$, compressibility, $\varkappa = dn/d\mu$, chemical potential, μ , ground-state energy density, $\mathcal{E}(n, k_0^2)$, as a function of n and the square of the superflow wavevector, k_0 , superfluid stiffness $n_s \equiv n_s(T=0) = 2\partial\mathcal{E}(n, k_0^2)/\partial(k_0^2)$, and higher-order derivatives ν , γ , and σ . The superfluid stiffness and superflow wavevector are the most convenient quantities to discuss the general case, especially lattice models. Unless stated otherwise, we will work in units where Planck's constant is set equal to unity. Our result, Eqs. (2)–(4), differs from the original Landau formula, [1]

$$\Delta n_s = -\frac{I_d}{d} \frac{(d+1)}{m^2 c(c\beta)^{d+1}}, \quad (5)$$

by a factor. In a Galilean system, both γ and σ have to be identically zero and $\nu = 1/m$. This is how Eqs. (2)–(4) recover the Landau expression, while revealing its quantitative and conceptual deficiency in a general case. Strictly speaking, both Landau theory and our generalized description may go beyond Eqs. (2)–(4) corresponding to the asymptotic regime when only the acoustic part of the phonon branch is excited. On the technical side, we derive Eqs. (2)–(4) starting from Popov's $(d+1)$ -dimensional hydrodynamic action based on the above-mentioned parameters and without invoking reference frame transformations.

As long as the gas of elementary excitations may be treated as non-interacting, Landau formula remains valid irrespective of the phonon dispersion relation, e.g. it correctly captures the roton contribution in ^4He . To achieve the same goal in the general case is far more challenging because one needs to include a large number of higher-order anharmonic terms.

The rest of the paper is organized as follows. In Sec. II, we consider mapping between the low-temperature d -dimensional quantum superfluid and $(d+1)$ -dimensional classical field system and how finite-temperature effects in the former relate to finite-size effects in the latter.

This allows us to introduce and study n_s depletion effects, both theoretically and numerically, in the simplified space-time symmetric case. Quantum case is discussed in Sec. III. Based on effective hydrodynamic Hamiltonian, we express Δn_s in terms of certain correlation functions. Calculating then the finite- T and finite-size contributions to these correlation functions—with bilinearized hydrodynamic action, we produce the desired results, including Eqs. (2)–(4). We validate the theory by performing quantum Monte Carlo simulations for several representative system of interacting bosons on the square lattice in Sec. IV. In Sec. V, we summarize our results and make concluding remarks—in particular, on how our approach can be straightforwardly generalized to reveal universal low-temperature thermodynamics of superfluids.

II. FINITE-SIZE EFFECTS IN A CLASSICAL U(1) SYSTEM

A. General analysis

Within the effective action formalism, the long-wave physics of a d -dimensional low-temperature quantum superfluid can be mapped onto that of a finite-size (along the imaginary-time direction) $(d+1)$ -dimensional classical counterpart. It is thus reasonable to put the problem in a somewhat broader context and first consider finite-size corrections to the superfluid stiffness in a simple $d_c = (d+1)$ classical XY -type model with broken U(1) symmetry and equivalence between all directions. Its effective long-wave action for the field of superfluid phase, $\Phi(r)$ is given by:

$$A[\Phi] = \int d^{d_c} r \left\{ \frac{\bar{\Lambda}_s}{2} (\nabla\Phi)^2 + \frac{\theta}{4} [(\nabla\Phi)^2]^2 \right\}, \quad (6)$$

(in the classical case, one can “absorb” temperature into the definition of coefficients and measure energies in units of temperature). Thermodynamically, parameter θ is defined through the second derivative of the free-energy density, \mathcal{F} , with respect to the square of the phase twist wavevector:

$$\theta = 2 \left. \frac{\partial^2 \mathcal{F}(k_0^2)}{\partial (k_0^2)^2} \right|_{k_0=0}. \quad (7)$$

In this sense, it is a direct analog of σ in the quantum case, see Eq. (4).

The value of $\bar{\Lambda}_s$ in the effective theory (6) depends on the small but finite UV momentum cutoff k_* so that $\bar{\Lambda}_s$ reaches its thermodynamic limit value Λ_s only in the $k_* \rightarrow 0$ limit. To the leading order, the difference between $\bar{\Lambda}_s$ and Λ_s comes from the quartic term inducing fluctuational corrections to $\bar{\Lambda}_s$. These corrections are also responsible for the finite-size (Casimir-type) effects on the value of Λ_s .

Two characteristic finite-size cases are particularly interesting. The first one is that of a hypercube sample

when all linear system sizes are equal. The second one corresponds to a finite linear size, L , in one direction only. This case describes finite-temperature depletion in an infinitely large quantum superfluid. We will see that here the answer is reminiscent of (2) with $\nu = 0$ and $c\beta$ replaced with L . An interesting fact that we demonstrate numerically is that the sign of θ can be both positive and negative, and can flip, as a function of control parameter(s), within one and the same simple statistical model.

Apart from two special cases, there are reasons to consider a more general setup with linear system size $L_{\parallel} = L$ in one special (“longitudinal”) direction, and L_{\perp} in all other directions. A convenient alternative parameterization of the sample geometry is through the aspect ratio:

$$\lambda = L/L_{\perp}. \quad (8)$$

The two special cases discussed above correspond to $\lambda = 1$ and $\lambda = 0$. Other values of the aspect ratio provide a tool for validation of the effective theory (6) and control over systematic errors in numeric data due to subleading corrections.

The finite-size effects have both qualitative and quantitative aspects. At the qualitative level, Λ_s becomes anisotropic at any $\lambda \neq 1$: The longitudinal, $\Lambda_s^{(\parallel)}(L, \lambda)$, and transverse, $\Lambda_s^{(\perp)}(L, \lambda)$, values deviate from Λ_s (and each other) due to different finite-size corrections: $\Delta\Lambda_s^{(\parallel)}(L, \lambda) \neq \Delta\Lambda_s^{(\perp)}(L, \lambda)$.

Superfluid stiffness components, $\Lambda_s^{(x)}$, in an anisotropic system are defined through linear response to the twisted boundary condition applied in the \hat{x} -direction:

$$\Lambda_s^{(x)} = -\frac{TL_x^2}{V} \frac{\partial^2 \ln Z}{\partial \varphi_0^2} \Big|_{\varphi_0=0} = -\frac{TL_x^2}{VZ} \frac{\partial^2 Z}{\partial \varphi_0^2} \Big|_{\varphi_0=0}. \quad (9)$$

Here φ_0 is the twist phase, V is the system volume, and Z is the partition function,

$$Z = \int \mathcal{D}\Phi e^{-A[\Phi]}. \quad (10)$$

In this paper, we consider low-temperature superfluids in $d \geq 2$ and their classical counterparts in $d_c \geq 3$, when contributions from phase-winding states are irrelevant for our analysis [10].

Imposing the twisted boundary condition on the field of phase, we have

$$\Phi = k_0 x + \varphi, \quad k_0 = \varphi_0/L_x. \quad (11)$$

Since contributions from states with 2π windings in φ are statistically negligible, terms linear in $\varphi_x \equiv \partial_x \varphi$ drop out from the action, and we have

$$\begin{aligned} \mathcal{A}(\nabla\Phi) &= \mathcal{A}(\nabla\varphi) + k_0^2 \left[\frac{\bar{\Lambda}_s}{2} + \theta \varphi_x^2 + \frac{\theta}{2} (\nabla\varphi)^2 \right] \\ &+ k_0 \theta (\nabla\varphi)^2 \varphi_x + \mathcal{O}(k_0^3). \end{aligned} \quad (12)$$

Terms mentioned in the second line of Eq. (12) prove irrelevant and will be omitted. $\mathcal{O}(k_0^3)$ terms do not contribute to the second-order derivative (9). Linear in k_0 term does produce a non-zero contribution to the free energy but this contribution is proportional to the second power of k_0 and thus is subleading (as a $1/L^2$ correction) to the contribution from quadratic in k_0 terms because it contains two extra derivatives.

Expansion in k_0^2 yields the expression

$$\Delta\Lambda_s^{(x)} = \frac{2\theta}{\Lambda_s} \Delta B + \frac{\theta}{\Lambda_s} \Delta C \quad (13)$$

for the depletion of the stiffness, where

$$B = \Lambda_s \langle \varphi_x^2 \rangle, \quad C = \Lambda_s \langle (\nabla\varphi)^2 \rangle. \quad (14)$$

Here we do not distinguish $\bar{\Lambda}_s$ and Λ_s by assuming that all expressions are UV-regularized. As opposed to the $\langle (\nabla\varphi)^2 \rangle$ average which is insensitive to the direction of the twist, finite-size corrections to $\langle \varphi_x^2 \rangle$ depend on whether the \hat{x} -direction is longitudinal or transverse. While it appears that we have three averages to compute: $\Delta B_{\parallel}(L, \lambda)$, $\Delta B_{\perp}(L, \lambda)$ and $\Delta C(L, \lambda)$, they are related following identity

$$\Delta C = \Delta B_{\parallel} + (d_c - 1) \Delta B_{\perp}. \quad (15)$$

In what follows, we will be expressing final answers in terms of ΔB_{\parallel} and ΔC :

$$\Delta\Lambda_s^{(\parallel)} = \frac{\theta}{\Lambda_s} (\Delta C + 2\Delta B_{\parallel}), \quad (16)$$

$$\begin{aligned} \Delta\Lambda_s^{(\perp)} &= \frac{\theta}{\Lambda_s} (\Delta C + 2\Delta B_{\perp}) \\ &= \frac{\theta}{(d_c - 1)\Lambda_s} [(d_c + 1)\Delta C - 2\Delta B_{\parallel}]. \end{aligned} \quad (17)$$

B. Results

1. General case

Being interested in the leading contributions, we calculate the averages based on the first (leading) term of the action (6). Calculations are readily performed in the Fourier representation (the mode with zero wavevector is gauged out):

$$\varphi(\mathbf{r}) = \frac{\lambda^{d_c-1}}{L^{d_c}} \sum_{\mathbf{k} \neq 0} \varphi_{\mathbf{k}} e^{i\mathbf{k} \cdot \mathbf{r}}, \quad (18)$$

$$\mathbf{k} \equiv \mathbf{k}_{\mathbf{n}} = \left(\frac{2\pi n_1}{L}, \frac{2\pi n_2}{L_{\perp}}, \dots, \frac{2\pi n_{d_c}}{L_{\perp}} \right). \quad (19)$$

Here $\mathbf{n} = (n_1, n_2, \dots, n_d)$ is an integer vector; without loss of generality, direction “1” is assumed to be the longitudinal direction.

In the Fourier representation, the average is given by

$$\langle |\varphi(\mathbf{k})|^2 \rangle = \frac{1}{n_s k^2}. \quad (20)$$

The next step is to write B and C as a sum over wavevectors. As discussed above, the effective action (6) implies a finite UV cutoff k_* , and hence the sums for B and C must be regularized by subtracting the corresponding integral with the same UV cutoff while replacing $\bar{\Lambda}_s$ with Λ_s . After regularization

$$\Delta C = \frac{\lambda^{d_c-1}}{L^{d_c}} \sum_{\mathbf{k} \neq 0} 1 - \int \frac{d^{d_c} k}{(2\pi)^{d_c}}, \quad (21)$$

$$\Delta B_{\parallel} = \frac{\lambda^{d_c-1}}{L^{d_c}} \sum_{\mathbf{k} \neq 0} \frac{k_1^2}{k^2} - \int \frac{d^{d_c} k}{(2\pi)^{d_c}} \frac{k_1^2}{k^2}. \quad (22)$$

Next we observe that the difference between the sum and integral in the r.h.s of Eq. (21) would yield identical zero if the sum contained the $\mathbf{k} = 0$ term (by considering 1 as the limiting case of a Gaussian with divergent width). Thus,

$$\Delta C = -\frac{\lambda^{d_c-1}}{L^{d_c}}. \quad (23)$$

In anticipation of the final answer for B_{\parallel} , we define the L -independent quantity

$$S_{\parallel}(\lambda) = L^{d_c} \Delta B_{\parallel}(L, \lambda). \quad (24)$$

and use dimensionless vector

$$\mathbf{q}_{\mathbf{n}} = (n_1, \lambda n_2, \dots, \lambda n_{d_c}), \quad (25)$$

to express the answer as

$$S_{\parallel} = \lambda^{d_c-1} \left[\sum_{\mathbf{n} \neq 0} \frac{n_1^2}{\mathbf{q}_{\mathbf{n}}^2} - \frac{1}{d_c} \int \frac{d^{d_c} q}{(2\pi)^{d_c}} \right] \quad (26)$$

(symmetrization of the integral in the r.h.s of (22) resulted in the prefactor $1/d_c$).

This way Eqs. (16)–(17) get converted in the following final answers:

$$\Delta \Lambda_s^{(\parallel)} = \frac{\theta/\Lambda_s}{L^{d_c}} [2S_{\parallel}(\lambda) - \lambda^{d_c-1}], \quad (27)$$

$$\Delta \Lambda_s^{(\perp)} = -\frac{\theta/\Lambda_s}{(d_c-1)L^{d_c}} [2S_{\parallel}(\lambda) + (d_c+1)\lambda^{d_c-1}]. \quad (28)$$

Equations (27) and (28) can be combined into relation

$$\theta = \frac{(d_c-1)\Lambda_s L^{d_c}}{2[d_c S_{\parallel}(\lambda) + \lambda^{d_c-1}]} [\Lambda_s^{(\parallel)} - \Lambda_s^{(\perp)}] \quad (29)$$

that proves very convenient for numeric validation of our theory by comparing its r.h.s. to the value of θ computed from derivatives of the free energy.

2. Hypercubic sample ($\lambda = 1$)

This case is particularly simple. Here we have $\Delta B_{\parallel} = \Delta B_{\perp}$, and from (15) and (23) we immediately see that

$$S_{\parallel}(\lambda = 1) = -\frac{1}{d_c} \quad (30)$$

and

$$\Delta \Lambda_s(L) = -\frac{(1+2/d_c)\theta}{\Lambda_s L^{d_c}}. \quad (31)$$

3. The $\lambda = 0$ limit

This case is of prime interest. We will not mention $\lambda = 0$ as an argument of functions throughout this section. Now the sum over n_2, n_3, \dots, n_{d_c} in Eq. (26) is replaced with the corresponding (d_c-1) -dimensional integral and the remaining sum over n_1 can be performed analytically. In Sec. A, we consider this and similar sums that emerge in the finite-temperature and finite-size expressions for Δn_s in the quantum case. Here we utilize Eqs. (A13), (A14), and (A15) for α_4 yielding

$$S_{\parallel} = -I_{d_c-1} \quad (\lambda = 0), \quad (32)$$

with I_d defined by (3). Hence,

$$\Delta \Lambda_s^{(\parallel)} = -2I_{d_c-1} \frac{\theta}{\Lambda_s L^{d_c}}, \quad (33)$$

$$\Delta \Lambda_s^{(\perp)} = \frac{2I_{d_c-1}}{d_c-1} \frac{\theta}{\Lambda_s L^{d_c}}, \quad (34)$$

and

$$\theta = \frac{(d_c-1)\Lambda_s L^{d_c}}{2d_c I_{d_c-1}} [\Lambda_s^{(\perp)}(L) - \Lambda_s^{(\parallel)}(L)]. \quad (35)$$

4. Sign of “depletion”

Since all corrections are proportional to θ their sign is controlled by the sign of θ , which, as we will see later, can flip within one and the same model as a function of control parameter(s). The other two circumstances controlling the sign are: (i) the aspect ratio λ and (ii) whether we are considering $\Delta \Lambda_s^{(\parallel)}$ or $\Delta \Lambda_s^{(\perp)}$. The hypercube case $\lambda = 1$ is particularly simple. Here $\Delta \Lambda_s^{(\parallel)} = \Delta \Lambda_s^{(\perp)} \equiv \Delta \Lambda_s$ and Eq. (31) tells us that the sign of depletion is always opposite to that of θ . The same is generically true for $\Delta \Lambda_s^{(\parallel)}$, which is seen from Eq. (33). The case of $\Delta \Lambda_s^{(\perp)}$ is more interesting. By comparing the $\lambda = 1$ and $\lambda = 0$ results, Eqs. (31) and (34), respectively, we conclude that the sign of $\Delta \Lambda_s^{(\perp)}$ as necessarily changes within the $\lambda \in (0, 1)$ interval.

C. Numeric simulations

The goal of numeric simulations is two-fold. First, we want to validate our analytic approach by comparing to controlled results for a simple model. One possibility is to compare data for θ obtained by two distinctively different ways: (i) employing thermodynamic relation (7) and (ii) deducing the value of θ from the finite-size effect, Eq. (35). As a by-product, we will also reveal the role of subleading corrections to the leading $\sim 1/L^{d_c}$ term. Our second goal is to demonstrate that the sign of θ can take both positive and negative values and even flip—as a function of control parameter—within one and the same single-parametric model.

1. The model

The simplest model to simulate is the J-current model

$$H_J/T = \frac{1}{2K} \sum_b \sum_{J_b} |J_b|, \quad J_b = -1, 0, +1. \quad (36)$$

Here b labels bonds of the d_c -dimensional hypercubic lattice, and J_b is the bond current that takes on three integer values. Allowed values of the bond currents are also required to obey the zero divergence constraint on each site. The model has a simple Pollock-Ceperley type [11] winding number estimator for θ based on Eq. (7), while $K > 0$ is the only control parameter of the model. For the model to be in the ordered state, K should be large enough. Our worm algorithm [12] simulations of the ordered state were performed in $d_c = 3$ dimensions at $K = 0.4$ and $K = 1.0$.

2. Winding number estimator for θ

Using

$$\mathcal{F} = -\frac{1}{V} \ln Z \quad (T = 1), \quad (37)$$

we have

$$\theta = \frac{2}{V} \left[\left(\frac{1}{Z} \frac{\partial Z}{\partial (k_0^2)} \right)^2 - \frac{1}{Z} \frac{\partial^2 Z}{\partial (k_0^2)^2} \right]_{k_0=0}.$$

To relate this expression to the statistics of winding numbers (cf. [11]), we rewrite it in terms of the phase twist φ_0 in the direction x [$k_0^2 = (\varphi_0/L_x)^2$]:

$$\theta = \frac{2L_x^4}{V} \left[\left(\frac{1}{Z} \frac{\partial Z}{\partial (\varphi_0^2)} \right)^2 - \frac{1}{Z} \frac{\partial^2 Z}{\partial (\varphi_0^2)^2} \right]_{\varphi_0=0}.$$

Expressing the full the partition function as the sum over winding numbers along the x -direction, W_x ,

$$Z = \sum_{W_x} Z_{W_x} e^{i\varphi_0 W_x} = \sum_{W_x} Z_{W_x} \cos(\varphi_0 W_x), \quad (38)$$

we see that

$$\frac{1}{Z} \frac{\partial Z}{\partial (\varphi_0^2)} \Big|_{\varphi_0=0} = -\frac{1}{2Z} \sum_{W_x} Z_{W_x} W_x^2 = -\frac{1}{2} \langle W_x^2 \rangle,$$

$$\frac{1}{Z} \frac{\partial^2 Z}{\partial (\varphi_0^2)^2} \Big|_{\varphi_0=0} = \frac{1}{12Z} \sum_{W_x} Z_{W_x} W_x^4 = \frac{1}{12} \langle W_x^4 \rangle,$$

and thus

$$\theta = \frac{L_x^4}{6V} [3 \langle W_x^2 \rangle^2 - \langle W_x^4 \rangle]. \quad (39)$$

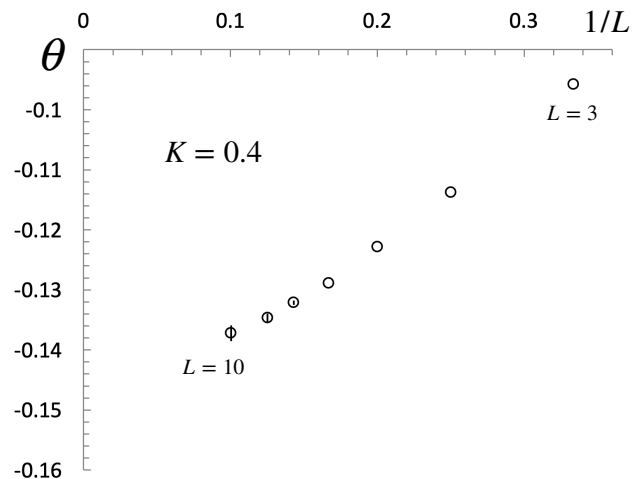


FIG. 1. Extracting parameter θ for the 3D J-current model (36) at $K = 0.4$ using estimator (39) for hypercubic samples of different sizes. The error bars are shown only for $L = 10, 8$ and 7 ; for $L < 7$, they are much smaller than the symbol size. Extrapolation to $L \rightarrow \infty$ yields $\theta = -0.14(1)$, which is consistent with the data for the Λ_s depletion shown in Figs. 3 and 2.

3. Numeric results

Simulations of the model (36) were performed for two values of K corresponding (respectively) to negative and positive sign of θ : $K = 0.4$ and $K = 1.0$.

The $K = 0.4$ data are presented in Figs. 1–2. Figure 1 shows results for θ as a function of system size when it is computed using Eq. (39). From this plot we deduce that $\theta = -0.145(1)$ with large systematic uncertainty coming from ambiguity of how the data should be extrapolated (see other examples and discussion below).

To verify Eqs. (27) and (28), we check their immediate implication—the prediction for θ , Eq. (29)—as a function of system size and aspect ratio by considering $\lambda \leq 1/2$. The values of $S_{\parallel}(\lambda)$ were calculated numerically using Eq. (26) with matching UV cutoffs for the sum and the integral. We find that $S_{\parallel}(0.5) \approx -0.382$, which is very

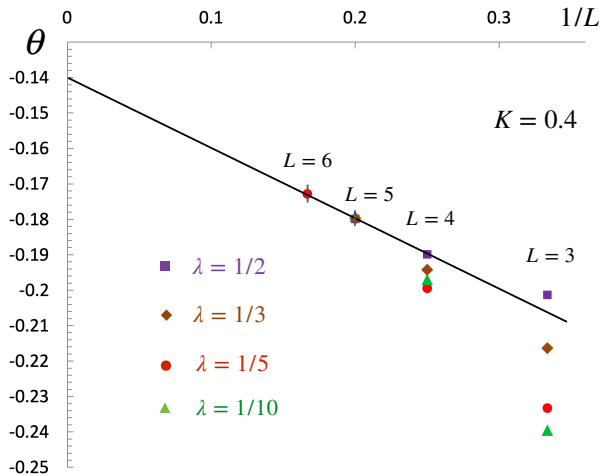


FIG. 2. Results for θ in the 3D J-current model (36) at $K = 0.4$ obtained for different system sizes and aspect ratios using relation (29). The error bars for samples with $L < 5$ are smaller than symbol size. Since at $L = 5$ the dependence on aspect ratio cannot be resolved within the error bars, simulation at $L = 6$ was performed only for $\lambda = 1/5$. The general trend is consistent with the thermodynamic limit result deduced from Fig. (1) and suggests that the subleading correction scales as $1/L$ (solid line fit).

close to the $\lambda = 0$ limit (32), implying that for $\lambda \leq 1/3$, the difference between the exact result and (32) is negligible.

Simulation results are presented in Fig. 2. For $L = 3$, results for different values of λ 's substantially deviate from the limiting value $\theta = -0.14$, as well as from each other. These deviations are dramatically reduced for $L = 4$, but remain pronounced. For $L = 5$ we can no longer resolve the dependence on aspect ratio within the error bars. Given that individual terms in (29) strongly depend on the aspect ratio, absence of such dependence for larger L , confirms the validity of our considerations in the thermodynamic limit. The data also suggest that the subleading correction to θ scales as $1/L$. Extrapolation of the ($\lambda = 0.5, L = 4, 5, 6$) set then leads to the estimate $\theta = 0.14(1)$, which we now use to validate the theory of depletion in the hypercube sample.

The data presented in Fig. 3 demonstrate that for the largest system sizes we correctly predict the leading term (31). Subleading contributions (we expect them to be proportional to $1/L^{(d_c+2)}$, see the text below Eq. (12)) start playing a role for system sizes $L \lesssim 10$, forcing us to consider them when fitting the data over a broader range of system sizes, see Fig. 3.

The main goal of the simulation at $K = 1.0$ is to reveal the sign change of θ (and $\Delta\Lambda_s$) as a function of control parameter K . The data presented in Figs. 4 and 5, clearly establish this fact. Somewhat unexpectedly (given system's behavior at $K = 0.4$), here we face a problem of independently extracting an accurate value of θ from the winding number estimator (39); see Fig. 4.

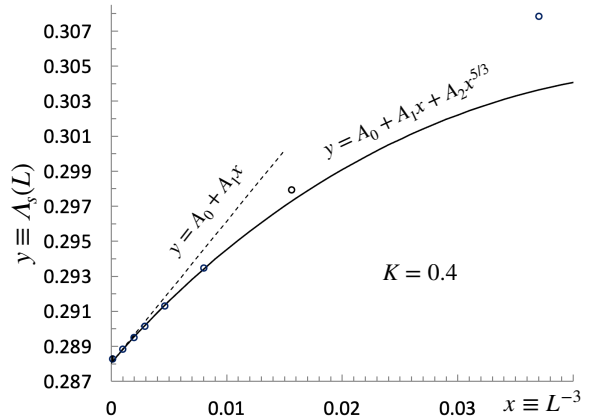


FIG. 3. Superfluid stiffness $\Lambda_s(L)$ of the 3D J-current model (36) at $K = 0.4$ for hypercubic samples with $L = 3, 4, 5, 6, 7, 8, 10, 20$. The error bar is shown only for $L = 20$; for other data points, the error bars are much smaller than the symbol size. We use the fitting ansatz $y(x) = A_0 + A_1x + A_2x^{5/3}$ (solid line) where the first two terms correspond to our theory and the subleading term is explained in the text. Parameters A_0 and A_2 ($A_0 = 0.28805$, $A_2 = 3.5$) are free fitting parameters while the value of A_1 is fixed by the relation (31), implying that $A_1 = -(5/3)\theta/\Lambda_s$, with $\Lambda_s \equiv A_0$, and independently measured $\theta = -0.14$, see Figs. 1 and 2. The fit demonstrates perfect consistency with prediction of Eq. (31). It also illustrates—by comparison with the asymptotic $y(x) = A_0 + A_1x$ law (dashed line)—that subleading contributions play significant role for system sizes $L \lesssim 10$.

The subleading corrections are not only strong but also non monotonic, dramatically changing the trend of finite-size effects at $L > 6$. Since large statistical errors prevent us from sampling larger system sizes, a reliable extrapolation to the thermodynamic limit is not possible. Nevertheless, the sign, the order-of-magnitude value, and the decreasing trend at $l \geq 7$ are qualitatively consistent with the value $\theta \approx 0.065$ value extracted from the fit in Fig. 5.

III. THE QUANTUM SYSTEM

Turning to the quantum system, we have two closely related but not identical options. From purely mathematical perspective, the most straightforward way to proceed is to start directly from Popov's hydrodynamic action, thereby immediately mapping the quantum d -dimensional problem onto the $(d+1)$ -dimensional pseudo-classical $U(1)$ model with complex-valued action. However, there is a subtlety. The Hydrodynamic action formalism works in the grand canonical ensemble while we are looking for the thermal depletion at a fixed density rather than than fixed chemical potential. That is why we prefer a somewhat different approach—a generalization of the approach previously used for the weakly interacting Bose gas [13]—that starts with hydrodynamic Hamiltonian.

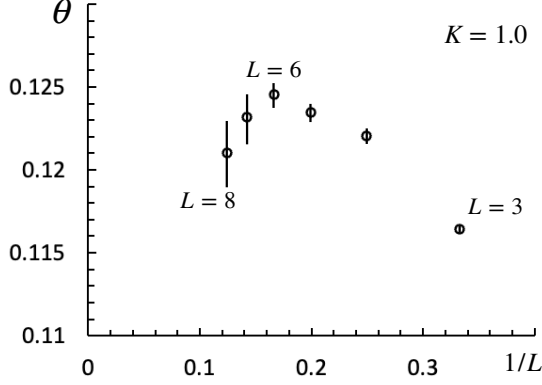


FIG. 4. Problem with extracting an accurate value of θ for the 3D J-current model (36) at $K = 1.0$ using estimator (39) for hypercubic samples. As opposed to the $K = 0.4$ case (see Fig. 1), radical change of the dependence on system size at $L = 6$ and rapidly increasing statistical errors for large L prevents us from making a reliable extrapolation to the thermodynamic limit, which according to the data shown in Fig. 5 is expected to be $\theta \approx 0.07$.

A. General analysis

The superfluid stiffness is the linear response coefficient relating supercurrent density (the expectation value of the persistent current density \mathbf{j}) to the (infinitesimal) value of \mathbf{k}_0 :

$$\langle \mathbf{j} \rangle = n_s \mathbf{k}_0 \quad (k_0 \rightarrow 0). \quad (40)$$

Current density in the long-wave limit is explicitly given by the derivative of the hydrodynamic Hamiltonian density over the phase gradient [13]:

$$\mathbf{j} = \frac{\partial \mathcal{H}(\eta, \nabla \Phi)}{\partial (\nabla \Phi)}. \quad (41)$$

Here $\mathcal{H}(\eta, \nabla \Phi)$ is a function of $\nabla \Phi$ and η , with η being the field of the number density fluctuations about the equilibrium expectation value n . By definition, $\mathbf{k}_0 = \langle \nabla \Phi \rangle$. The hydrodynamic Hamiltonian is obtained by expanding the ground state energy density, $\mathcal{E}(n, k_0^2)$, in powers of η and k_0^2 , with subsequent substitution $k_0^2 \rightarrow (\nabla \Phi)^2$ [13]. Up to irrelevant for our purposes higher-order terms, the hydrodynamic Hamiltonian reads

$$\begin{aligned} \mathcal{H}(\eta, \nabla \Phi) = & \frac{n_s^{(0)}}{2} (\nabla \Phi)^2 + \frac{\eta^2}{2\kappa} + \frac{\nu\eta}{2} (\nabla \Phi)^2 \\ & + \frac{\gamma\eta^2}{2} (\nabla \Phi)^2 + \frac{\sigma}{4} (\nabla \Phi)^4. \end{aligned} \quad (42)$$

Compared to the simple classical effective action discussed in previous section, the hydrodynamic Hamiltonian features several additional physical parameters;

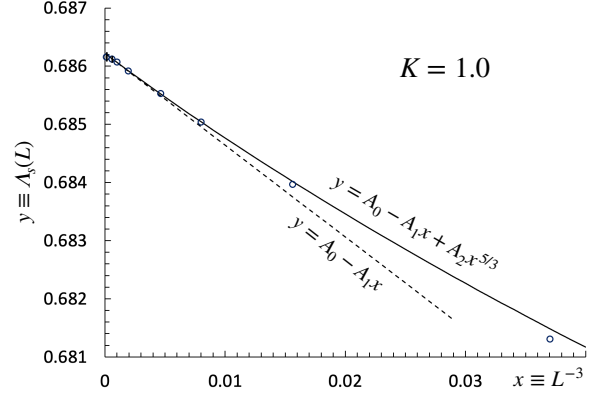


FIG. 5. Superfluid stiffness $\Lambda_s(L)$ for hypercubic samples of the 3D J-current model (36) at $K = 1.0$. The error bars are shown only for system sizes $L = 20$ and 12 ; they are much smaller than the symbol size for $L < 12$. Similar to Fig. 3, we use the fitting ansatz $y(x) = A_0 - A_1x + A_2x^{5/3}$ (solid line), but now with θ being a free fitting parameter in addition to A_0 and A_2 ; the result is ($\theta = 0.065$, $A_0 = 0.68622$, $A_2 = 0.27$). In practice, A_0 is known very accurately from the largest system size simulation ($A_0 \approx \Lambda_s(L = 20) = 0.6862$), and thus A_1 is directly related to θ by the relation $A_1 = -(5/3)\theta/\Lambda_s$, see Eq. (31). The dashed line, $y(x) = A_0 - A_1x$, corresponds to the asymptotic linear behavior.

their meaning was described in the Introduction below Eqs. (2)–(4). According to Eqs. (41) and (42) the current density is given by

$$\mathbf{j} = n_s^{(0)} \nabla \Phi + \nu\eta \nabla \Phi + \gamma\eta^2 \nabla \Phi + \sigma (\nabla \Phi)^2 \nabla \Phi. \quad (43)$$

To proceed, we separate the superflow phase gradient from phase fluctuations,

$$\Phi = k_0 x + \varphi, \quad (44)$$

and assume without loss of generality that $\mathbf{k}_0 = k_0 \hat{\mathbf{x}}$. The bi-linear (in terms of density and phase fluctuations) Hamiltonian reads

$$\mathcal{H}(\eta, \nabla \varphi) = \frac{n_s^{(0)}}{2} (\nabla \varphi)^2 + \frac{\eta^2}{2\kappa} + k_0 \nu \eta \varphi_x. \quad (45)$$

As we will see, the higher-order terms prove irrelevant as long as we deal with the canonical ensemble. Again, since φ is periodic in the x -direction, we can safely omit the term $n_s^{(0)} \mathbf{k}_0 \cdot \nabla \varphi$ from the Hamiltonian density (45) because it has zero contribution to the action. In terms of our parameterization, the x -component of the current density operator is (omitting terms $\propto k_0^2$)

$$\begin{aligned} j_x = & n_s^{(0)} k_0 + k_0 [\gamma\eta^2 + 2\sigma\varphi_x^2 + \sigma(\nabla\varphi)^2] + \nu\eta\varphi_x \\ & + n_s^{(0)} \varphi_x + \nu k_0 \eta + \sigma(\nabla\varphi)^2 \varphi_x. \end{aligned} \quad (46)$$

All terms in the second line of Eq. (46) vanish upon averaging with the bi-linear Hamiltonian (45) because they

are based on odd powers of fluctuating fields. The omission of the second term in the second line is the key circumstance distinguishing the canonical ensemble from the grand canonical one. In the latter case, this term would generate two extra relevant contributions: one coming from the term $\propto \eta(\nabla\Phi)^2$ shown in the Hamiltonian (42) and another one from the term $\propto \eta^3$ [not shown in (42) in view of its irrelevance as long as we look for the depletion at constant density. The averages of the terms in the first line of Eq. (46) do not depend—in the leading order—on whether we calculate them in the canonical or grand canonical ensemble.

The temperature-induced change of the superfluid stiffness at a fixed number density thus comes as a sum of three terms (with appropriate UV regularization similarly to the classical case):

$$\Delta n_s = \Delta n_s^{(\nu)} + \Delta n_s^{(\gamma)} + \Delta n_s^{(\sigma)}, \quad (47)$$

$$\Delta n_s^{(\nu)} = \nu \lim_{k_0 \rightarrow 0} \frac{\langle \eta \varphi_x \rangle}{k_0} = \nu \left. \frac{\partial \langle \eta \varphi_x \rangle}{\partial k_0} \right|_{k_0=0}, \quad (48)$$

$$\Delta n_s^{(\gamma)} = \gamma \langle \eta^2 \rangle, \quad \Delta n_s^{(\sigma)} = \sigma \langle (\nabla \varphi)^2 \rangle + 2\sigma \langle \varphi_x^2 \rangle. \quad (49)$$

As long as averages in Eqs. (48) and (49) do not vanish at $T = 0$ —in which case they have to be k_* -dependent—their $T = 0$ contributions should be considered as quantum renormalization of the k_* -dependent $n_s^{(0)}$ value converting it to the genuine ground-state value of n_s , and, therefore, subtracted from the final answer for Δn_s . We will see that $\Delta n_s^{(\nu)}(\beta \rightarrow \infty) \rightarrow 0$, while it is clear that $\Delta n_s^{(\gamma)}$ and $n_s^{(\sigma)}$ remain finite in the zero temperature limit.

Evaluation of averages in Eqs. (48) and (49) is done straightforwardly within the Popov's hydrodynamic action with the bi-linear Hamiltonian density [14] ($\dot{\varphi} \equiv \partial_\tau \varphi$, $\beta = 1/T$)

$$S = \int_0^\beta d\tau \mathcal{L}(\eta, \dot{\varphi}, \nabla \varphi), \quad \mathcal{L} = -i\eta \dot{\varphi} - \mathcal{H}. \quad (50)$$

We illustrate the procedure by considering the average (48) as the most sophisticated one among the rest. A convenient trick is to introduce the source term

$$\mathcal{L} \rightarrow \mathcal{L} + \alpha \eta \varphi_x, \quad (51)$$

in order to express the average in (48) through derivatives of the partition function logarithm. This way (48) reduces to (V is the system's volume)

$$\Delta n_s^{(\nu)}(\beta) = \frac{\nu}{\beta V} \left. \frac{\partial^2 \ln Z}{\partial k_0 \partial \alpha} \right|_{\alpha=k_0=0}, \quad (52)$$

$$Z = \int e^{S[\eta, \varphi]} \mathcal{D}\eta \mathcal{D}\varphi = \text{const} \int e^{S_\varphi[\varphi]} \mathcal{D}\varphi. \quad (53)$$

Action $S_\varphi[\varphi]$ is readily obtained by integrating out the Gaussian η -field; its Lagrangian density (up to irrelevant higher-order terms, and, in particular, terms $\propto \alpha^2$ and $\propto k_0^2$) is

$$\mathcal{L}_\varphi = \mathcal{L}_\varphi^{(0)} + \mathcal{L}_\varphi^{(1)}, \quad (54)$$

$$\mathcal{L}_\varphi^{(0)} = -\frac{\varkappa}{2} \dot{\varphi}^2 - \frac{n_s^{(0)}}{2} (\nabla \varphi)^2, \quad (55)$$

$$\mathcal{L}_\varphi^{(1)} = i(\nu k_0 - \alpha) \varkappa \dot{\varphi} \varphi_x - \varkappa \nu k_0 \alpha \varphi_x^2. \quad (56)$$

This brings us to the following expression

$$\Delta n_s^{(\nu)} = \nu^2 \left[\varkappa^2 \int d\tau d^d r \mathcal{K}(\mathbf{r}, \tau) - \varkappa \langle \varphi_x^2 \rangle \right], \quad (57)$$

$$\mathcal{K}(\mathbf{r}, \tau) = \langle \dot{\varphi}(\mathbf{r}, \tau) \varphi_x(\mathbf{r}, \tau) \dot{\varphi}(0, 0) \varphi_x(0, 0) \rangle_0, \quad (58)$$

where the average is taken with respect to the action $S_0 = \iint d\tau d^d r \mathcal{L}_\varphi^{(0)}$. Evaluation of the correlator $\mathcal{K}(\mathbf{r}, \tau)$ is straightforward due to the Gaussian character of S_0 . The first step is applying Wick's theorem with the observation that $\langle \varphi_x(\mathbf{r}, \tau) \dot{\varphi}(\mathbf{r}, \tau) \rangle = \langle \varphi_x(0, 0) \dot{\varphi}(0, 0) \rangle = 0$ by $x \rightarrow -x$ and $\tau \rightarrow -\tau$ symmetries. This yields

$$\begin{aligned} \mathcal{K}(\mathbf{r}, \tau) &= \langle \dot{\varphi}(\mathbf{r}, \tau) \dot{\varphi}(0, 0) \rangle_0 \langle \varphi_x(\mathbf{r}, \tau) \varphi_x(0, 0) \rangle_0 \\ &\quad + \langle \dot{\varphi}(\mathbf{r}, \tau) \varphi_x(0, 0) \rangle_0 \langle \varphi_x(\mathbf{r}, \tau) \dot{\varphi}(0, 0) \rangle_0, \end{aligned} \quad (59)$$

thereby reducing the problem to the product of two standard phase-phase correlators $\langle \varphi(\mathbf{r}, \tau) \varphi(0, 0) \rangle_0$ differentiated with respect to either τ and/or x .

Thus, the answer for Δn_s comes in the form of finite- β corrections, ΔA , ΔB , ΔC and ΔD to the correlators

$$A = \varkappa^2 \int d\tau d^d r \mathcal{K}(\mathbf{r}, \tau), \quad (60)$$

$$B = \varkappa \langle \varphi_x^2 \rangle, \quad C = \varkappa \langle (\nabla \varphi)^2 \rangle, \quad D = \frac{\varkappa}{c^2} \langle \dot{\varphi}^2 \rangle, \quad (61)$$

where we have taken into account $\eta = -i\varkappa \dot{\varphi}$. Specifically, we have

$$\Delta n_s = \nu^2 (\Delta A - \Delta B) + \frac{2\sigma}{\varkappa} \Delta B + \frac{\sigma}{\varkappa} \Delta C - \gamma n_s \Delta D. \quad (62)$$

One can literally “read off the page” the phase-phase correlator in Fourier space by looking at Eq. (55):

$$\langle |\varphi_{\mathbf{k}, \omega}|^2 \rangle = \frac{1}{\varkappa \omega^2 + n_s k^2}. \quad (63)$$

Here ω stands for bosonic Matsubara frequency. With rescaling by the velocity of sound, $c\beta$ plays the role of an extra spatial dimension in the harmonic action. Hence, it is convenient to introduce the “imaginary-time wavevector”

$$\zeta \equiv \omega/c. \quad (64)$$

What is left is evaluation of explicit expressions for A , B , C and D :

$$A = \frac{2}{c^2\beta V} \sum_{\mathbf{k}, \zeta} \frac{k_x^2 \zeta^2}{(\zeta^2 + k^2)^2}, \quad (65)$$

$$B = \frac{1}{c^2\beta V} \sum_{\mathbf{k}, \zeta} \frac{k_x^2}{\zeta^2 + k^2}, \quad C = \frac{1}{c^2\beta V} \sum_{\mathbf{k}, \zeta} \frac{k^2}{\zeta^2 + k^2}, \quad (66)$$

$$D = \frac{1}{c^2\beta V} \sum_{\mathbf{k}, \zeta} \frac{\zeta^2}{\zeta^2 + k^2}. \quad (67)$$

The structure of Eq. (62) reveals similarities with the classical system. Calculating the finite-temperature correction to n_s is completely analogous to computing the finite-size correction (by discretization of the corresponding wavevector values). Thus, the problem is mathematically equivalent to that of an anisotropic classical system, this time with *three* inequivalent directions.

Similar to the calculations in Sec. II, we will assume that the $\mathbf{k}, \omega = 0$ mode has been subtracted from the Fourier expansion of the field $\varphi(\mathbf{r}, \tau)$. With this particular choice of “gauge”, we can write ΔD in terms of ΔC as

$$\Delta D = -\frac{1}{c^2\beta V} - \Delta C, \quad (68)$$

reducing the number of correlators to be calculated to three. Note that the first term on the right hand side of Eq. (68) vanishes if at least one of the linear system sizes is taken to infinity, or if temperature is set to zero.

The calculation of the correlators A , B and C involves explicitly evaluating certain standard sums and integrals. The problem reduces to evaluating four coefficients $\alpha_1, \dots, \alpha_4$. We refer to Appendix A for the mathematical details, and will in the rest of this section directly present results of the calculations for certain cases of interest.

B. Finite-temperature corrections

This case is of main interest because it directly brings us to the generalization of Landau formula (2) for the superfluid stiffness depletion. For finite β and infinite spatial directions, the only discrete wavevector in (65)–(66) is ζ . After symmetrization of the integrand and replacement k_x^2 with k^2/d , we introduce a dimensionless wavevector \mathbf{q}

$$\mathbf{q} = c\beta\mathbf{k}, \quad (69)$$

and observe, using Eqs. (A3), (A6), (A10) and (A12), that

$$c(c\beta)^{d+1}\Delta A(\beta) = \frac{2}{d}\alpha_3 = -I_d, \quad (70)$$

$$c(c\beta)^{d+1}\Delta B(\beta) = \frac{1}{d}\alpha_1 = \frac{I_d}{d}, \quad (71)$$

$$c(c\beta)^{d+1}\Delta C(\beta) = \alpha_1 = I_d. \quad (72)$$

Hence, the finite- β depletion of n_s is given by

$$\frac{c(\beta c)^{d+1}\Delta n_s(\beta)}{I_d} = -\frac{d+1}{d}\nu^2 + \frac{d+2}{d}\frac{\sigma}{\varkappa} + \gamma n_s. \quad (73)$$

C. Finite-size corrections

Assume now that the linear system size in one of the directions, call it the \hat{f} -direction, be finite and equal to L (with the periodic boundary condition implied), while in other directions systems sizes and β are infinite. In this situation n_s becomes anisotropic: the longitudinal (along \hat{f} -direction), and transverse values of the superfluid stiffness are now different due to finite-size corrections: $\Delta n_s^{(\parallel)}(L) \neq \Delta n_s^{(\perp)}(L)$. As in the classical system, the phase fluctuations depend on whether the directions \hat{f} and \hat{x} are parallel or orthogonal: $\Delta A_{\parallel}(L) \neq \Delta A_{\perp}(L)$ and $\Delta B_{\parallel}(L) \neq \Delta B_{\perp}(L)$. [Note that $\Delta C(L)$ remains isotropic by the spatial symmetry of the sum in Eq. (66).]

The sum for $\Delta A_{\parallel}(L)$ is identical to that for $\Delta A(\beta)$ in an infinite system—up to swapping τ and x variables places and rescaling by the sound velocity. A direct analog of (70) reads:

$$cL^{d+1}\Delta A_{\parallel}(L) = \frac{2}{d}\alpha_3 = -I_d. \quad (74)$$

Exactly the same considerations apply to $\Delta B_{\perp}(L)$:

$$cL^{d+1}\Delta B_{\perp}(L) = \frac{1}{d}\alpha_1 = \frac{I_d}{d}. \quad (75)$$

Sums for $\Delta A_{\perp}(L)$ and $\Delta B_{\parallel}(L)$ do not have finite- T analogs. In the case of $\Delta B_{\parallel}(L)$, we substitute

$$k_x = 2\pi n/L, \quad n = 0, \pm 1, \pm 2, \dots, \quad (76)$$

in to Eq. (66) and observe that the calculation reduces to that of the α_4 coefficient in Appendix A. Using Eqs. (A13) and (A15), we have

$$cL^{d+1}\Delta B_{\parallel}(L) = \alpha_4 = -I_d, \quad (77)$$

Likewise, to calculate $\Delta A_{\perp}(L)$, we substitute

$$k_f = 2\pi n/L, \quad n = 0, \pm 1, \pm 2, \dots, \quad (78)$$

in to Eq. (65) to map the calculation to that of the α_2 coefficient in Appendix A, resulting in

$$cL^{d+1}\Delta A_{\perp}(L) = \frac{2}{d(d+2)}\alpha_2 = \frac{I_d}{d}. \quad (79)$$

Note that in integrals over the space of $\mathbf{q} = (q_1, q_2, q_3, \dots, q_d)$ a factor $q_1^2 q_2^2$ can be converted into $q^4/[d(d+2)]$ upon hyper-angle averaging, see Appendix B. Finally, since isotropic ΔC is trivially decomposed into B-sums

$$\Delta C = (d-1)B_\perp(L) + B_\parallel(L), \quad (80)$$

we have

$$cL^{d+1}\Delta C = -\frac{I_d}{d}. \quad (81)$$

This brings us to the results

$$\frac{cL^{d+1}\Delta n_s^{(\parallel)}(L)}{I_d} = -\frac{(2d+1)\sigma}{d\kappa} - \frac{\gamma n_s}{d}, \quad (82)$$

$$\frac{cL^{d+1}\Delta n_s^{(\perp)}(L)}{I_d} = \frac{\sigma}{d\kappa} - \frac{\gamma n_s}{d}. \quad (83)$$

Independence of finite-size corrections on $\nu = dn_s/dn$ might appear surprising. Nevertheless, this outcome can be immediately deduced—by contradiction—from Landau theory of superfluidity in a Galilean system. For such a system, $\gamma = \sigma = 0$, while $\nu = 1/m \neq 0$, and existence of a ν -dependent finite-size correction would imply dependence of ground-state stiffness on L , in contradiction with the fact that in a Galilean system $n_s(T=0) \equiv n$, no matter whether the system size is infinite or finite.

Similarly to Eq. (35), an expression for σ in terms of $\Delta n_s^{(\parallel)}$ and $\Delta n_s^{(\perp)}$ can be obtained by subtracting Eq. (82) from Eq. (83), resulting in

$$\sigma = \frac{d\kappa cL^{d+1}}{2I_d(d+1)}(n_s^{(\perp)} - n_s^{(\parallel)}). \quad (84)$$

This expression serves as a useful numeric check against Eq. (97), since $n_s^{(\parallel)}$ and $n_s^{(\perp)}$ can easily be obtained from simulations of anisotropic systems by sampling winding numbers in different spatial directions.

D. Finite temperature and system size

In numeric simulations, both $c\beta$ and linear system size(s) are finite and not necessarily equal to each other. Let us consider a typical case of a spatial hypercube with linear size L . Following treatment similar to that in Sec. II, we define the dimensionless ratio

$$\lambda_\beta = \frac{c\beta}{L}, \quad (85)$$

so that all results can be expressed as functions of (β, λ_β) .

Now all wavevectors are discrete and given by

$$\zeta = \frac{2\pi n_0}{c\beta}, \quad k_i = \frac{2\pi n_i}{L} \quad (i \neq 0), \quad (86)$$

where n_0 and n_i are integers. Defining the $(d+1)$ -dimensional vectors

$$\mathbf{n} = (n_0, n_1, n_2, \dots, n_d) \quad (87)$$

and

$$\mathbf{q}_\mathbf{n} = (\lambda_\beta^{-1}n_0, n_1, \dots, n_d), \quad (88)$$

the regularized sums for ΔA , ΔB , and ΔC , upon symmetrization of the integrals, take the form

$$\Delta A = \frac{\lambda_\beta^d}{c(c\beta)^{d+1}} \left(\lambda_\beta^{-2} \sum_{\mathbf{n}} \frac{n_0^2 n_1^2}{\mathbf{q}_\mathbf{n}^4} - \frac{1}{(d+1)(d+3)} \int d^{(d+1)}q \right), \quad (89)$$

$$\Delta B = \frac{\lambda_\beta^d}{c(c\beta)^{d+1}} \left(\sum_{\mathbf{n}} \frac{n_1^2}{\mathbf{q}_\mathbf{n}^2} - \frac{1}{d+1} \int d^{(d+1)}q \right), \quad (90)$$

$$\Delta C = d\Delta B, \quad (91)$$

$$\Delta D = -\frac{\lambda_\beta^d}{c(c\beta)^{d+1}} - d\Delta B \quad (92)$$

Eq. (91) immediately follows from Eq. (66) by isotropy in spatial directions, while Eq. (92) follows from combining Eq. (68) and Eq. (91). For details of the symmetrization procedure leading to the prefactor in front of the integral appearing in Eq. (89), see Appendix B.

E. Spacetime hypercube at $\nu = 0$

Of special interest and importance for our numeric simulations (see below) is the case of spacetime hypercube ($c\beta = L$) at $\nu = 0$, which is quite similar to the $\lambda = 1$ case in the classical model (6).

At $\nu = 0$ there is no contribution from ΔA . The remaining terms ΔB and ΔC are easily mapped to those appearing in the calculation for the classical system. Thus, we end up with the formula

$$c(c\beta)^{d+1}\Delta n_s = \frac{\gamma n_s}{d+1} - \frac{(2+d)\sigma}{(d+1)\kappa} \quad (c\beta = L, \nu = 0). \quad (93)$$

A notable feature of Eq. (93) is that if the parameter σ is negative and large enough in modulus, it is possible to observe an increase of the superfluid stiffness as temperature is increased and the system size is decreased, while keeping $c\beta = L$.

IV. NUMERICS

A. Estimators

All quantities involved in the theory can be extracted from Worm Algorithm path-integral Monte Carlo simulations [15, 16] performed in the Grand canonical ensemble at low temperature in systems of finite size L . [In what follows all expressions refer to systems with the same size in all dimensions; i.e. the system volume is $V = L^d$.] If $P(N, \mathbf{M})$ is the probability of having a state with the particle number N , and winding number \mathbf{M} (it is a d -dimensional vector) then

$$n = V^{-1} \sum_{N\mathbf{M}} NP(N, \mathbf{M}) \equiv \frac{1}{V} \langle N \rangle, \quad (94)$$

$$\varkappa = \frac{1}{TV} \langle [N - \langle N \rangle]^2 \rangle, \quad (95)$$

$$n_s = \frac{TL^{2-d}}{d} \langle \mathbf{M}^2 \rangle. \quad (96)$$

While it is possible to derive estimators also for ν and γ , in practice it is much easier to estimate them in a large system by performing a numerical derivative based on simulations at different densities. Numerical derivative is obviously less accurate than n_s itself, but there is no problem in obtaining it with a few percent accuracy.

Turning to the estimator for the parameter σ , we note that the estimator

$$\tilde{\sigma} = \frac{TL^{4-d}}{6d} \sum_{\alpha=1}^d [3\langle \mathbf{M}_\alpha^2 \rangle^2 - \langle \mathbf{M}_\alpha^4 \rangle] \quad (97)$$

[a direct analog of the estimator (39) for the parameter θ of the classical model] produces a somewhat different quantity. This is because the worm algorithm used for simulations works in the grand canonical ensemble. In this case, we get

$$\tilde{\sigma} = \frac{2}{V} \left. \frac{\partial^2 \Omega(\mu, k_0^2)}{\partial (k_0^2)^2} \right|_{k_0=0} = \left. \frac{\partial n_s(\mu, k_0^2)}{\partial (k_0^2)} \right|_{k_0=0} \quad (98)$$

(Ω is the grand canonical potential, k_0 has the same meaning as before), which is different from

$$\sigma = \left. \frac{\partial n_s(n, k_0^2)}{\partial (k_0^2)} \right|_{k_0=0} \quad (99)$$

and thus needs to be related to σ and other previously introduced parameters. This is conveniently done with the Jacobian technique:

$$\frac{\partial n_s(n, k_0^2)}{\partial (k_0^2)} = \frac{\mathcal{D}(n_s, \mu)}{\mathcal{D}(k_0^2, \mu)} = \frac{\mathcal{D}(n_s, \mu)}{\mathcal{D}(k_0^2, n)} \left[\frac{\mathcal{D}(k_0^2, \mu)}{\mathcal{D}(k_0^2, n)} \right]^{-1}.$$

Observing/recalling that

$$\left. \frac{\partial n_s(n, k_0^2)}{\partial n} \right|_{k_0=0} = \nu, \quad \left. \frac{\partial n_s(n, k_0^2)}{\partial (k_0^2)} \right|_{k_0=0} = \sigma,$$

$$\begin{aligned} \left. \frac{\partial \mu(n, k_0^2)}{\partial (k_0^2)} \right|_{k_0=0} &= \left. \frac{\partial^2 \mathcal{E}(n, k_0^2)}{\partial n \partial (k_0^2)} \right|_{k_0=0} \\ &= \frac{1}{2} \left. \frac{\partial n_s(n, k_0^2)}{\partial n} \right|_{k_0=0} = \frac{\nu}{2}, \end{aligned}$$

$$\left. \frac{\partial \mu(n, k_0^2)}{\partial n} \right|_{k_0=0} = \varkappa^{-1},$$

$$\left[\frac{\mathcal{D}(k_0^2, \mu)}{\mathcal{D}(k_0^2, n)} \right]^{-1} = \left. \frac{\partial n(\mu, k_0^2)}{\partial \mu} \right|_{k_0=0} = \varkappa,$$

we conclude that

$$\tilde{\sigma} = \sigma - \varkappa \nu^2 / 2. \quad (100)$$

The estimator for the parameter $\tilde{\sigma}$ also involves precise cancellation of large terms. Given that winding number fluctuations themselves scale according to (96), the required relative accuracy of computing each average in (97) must be much smaller than

$$\epsilon \sim \frac{\tilde{\sigma}}{TL^{4-d}} \left(\frac{mTL^{2-d}}{n_s} \right)^2 \sim \frac{\tilde{\sigma} m^2}{n_s^2} \frac{1}{\beta V}. \quad (101)$$

This result implies that even if simulations are based on a “perfect” Monte Carlo algorithm (with autocorrelation time equal to one sweep, or $\propto V\beta$ updates) the required number of updates scales as the $(d+1)$ -dimensional system volume cubed. Fortunately, in this work we are interested in properties of the superfluid phase close to the ground state and thus small system sizes $L < 10$ can be used for computing $\tilde{\sigma}$.

B. Model

In our simulations, we employ the microscopic Hamiltonian

$$H = -t \sum_{\langle i,j \rangle} (c_i^\dagger c_j + \text{H.c.}) + U \sum_i n_i^2 - \mu \sum_i n_i, \quad (102)$$

of the Bose-Hubbard model. Here c_i^\dagger and c_i are bosonic creation and annihilation operators respectively, and $n_i = c_i^\dagger c_i$. All simulations are performed in two spatial dimensions on the square lattice. At low temperature the Hamiltonian (102) exhibits superfluidity. Because of the lack of continuous translation invariance, the depletion will not be described by Landau theory, but instead by the more general expression (62).

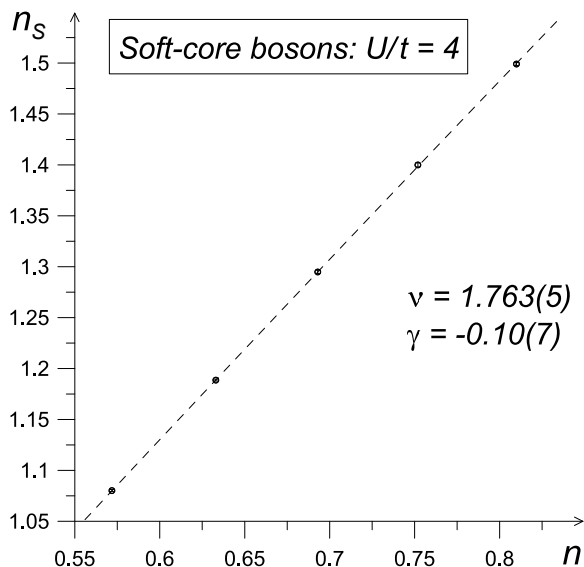


FIG. 6. Superfluid stiffness as a function of density for soft-core bosons in 2D with $U/t = 4$ (for system size $L \times L = 64 \times 64$ and $\beta/t = 6$). Dashed curve is a parabolic fit with $\nu = 1.763(5)ta^2$ and $\gamma = 0.10(7)ta^4$. Error bars are smaller than symbol sizes.

C. Soft-core bosons

At generic filling factor and at moderate values of on-site repulsion, we have a system of superfluid soft-core bosons. In this case, the largest parameter controlling the superfluid density depletion with temperature in Eq. (2) is coming from large ν . From the accurate data for $n_s(n)$ dependence, see Fig. 6, we extract the value of ν , which in this case is large but still significantly different from the Galilean invariant result $\nu = 2ta^2$. In sharp contrast with the hard-core system considered in the next subsection, the coefficient γ happens to be very small for this parameter regime and within the accuracy of our simulations may be set to zero.

For study of finite-temperature effects, we consider system density $n \approx 0.693$ characterized by compressibility $\varkappa = 0.2974(5)t$ and sound velocity $c = 2.087(3)ta$. It turned out that simulations of soft-core bosons are very demanding: the $\tilde{\sigma}$ parameter can be computed only for system sizes $L \leq 6$. The estimate of $\tilde{\sigma}$ (using small system sizes) from moments of the winding number distribution, Eq. (97), is $\tilde{\sigma}(L = 6) \approx -0.60(10)t$. This result implies that $\sigma = -0.15(10)$. In Fig. 7 we compare computed $n_s(T)$ dependence with the fit-free theoretical prediction based on Eq. (2) and $\sigma = -0.1$. The agreement is near perfect, i.e. within error bars for all points.

D. Hard-core bosons

If the limit $U \rightarrow \infty$ is taken in the Bose-Hubbard Hamiltonian (102), we acquire the so-called *hard-core bo-*

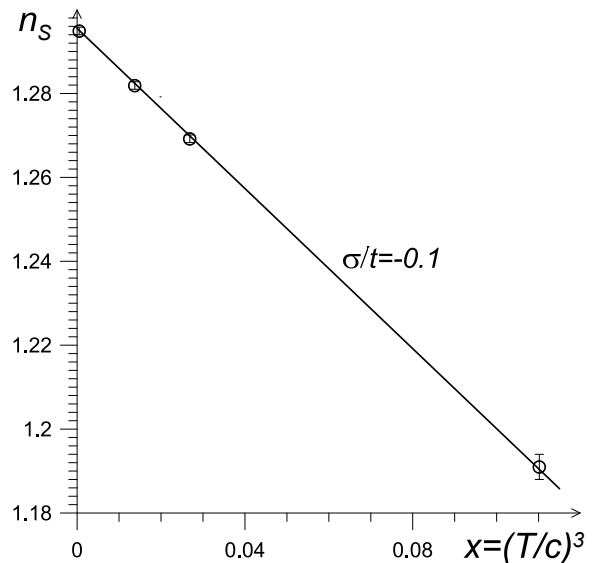


FIG. 7. Superfluid stiffness depletion as a function of $x = (cT)^3$ for soft-core bosons in 2D with $U/t = 4$ (for system size $L \times L = 64 \times 64$). Solid (black) curve is the $f(x) = A + Bx$ theoretical prediction with $A = n_s(T = t/6)$ and B fixed by the measured system parameters according to Eq. (2).

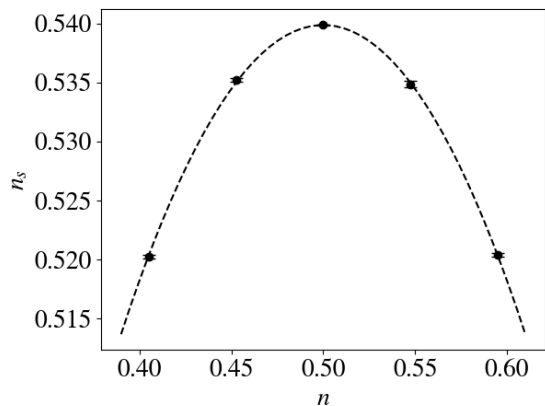


FIG. 8. Superfluid stiffness as a function of density for a hard-core boson system with $L = c\beta = 10$. Parameter γ is calculated with a quadratic fit, which yields $\gamma = -2.14(1)ta^4$ when extrapolated to $T = 0$.

son model. At half-filling ($\mu = 0$), this model is particle-hole symmetric, meaning that the parameter ν appearing in Eq. (2) is identically zero. Unlike the soft-core bosons, the parameter γ is not negligible in the hard-core system. We extract γ by fitting a quadratic to $n_s(n)$ data as shown in Fig. 8, yielding $\gamma = -2.14(1)ta^4$ when extrapolating to $T = 0$. Using the estimators in Sec. IV, we compute for the hard-core system $c = 2.2688(3)ta$ and $\varkappa = 0.10476(1)t$.

For the hard-core system, deviations from the T^3 -law happen at lower temperatures than in the soft-core sys-

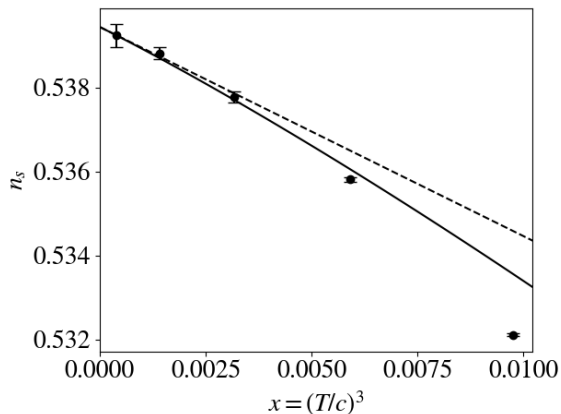


FIG. 9. Finite-temperature depletion of superfluid stiffness in the 2D system of hard-core bosons. System size was chosen such that the aspect ratio $L/c\beta \approx 4.698$ for all data points. Solid line is a fit of the function $f(x) = A_0 + A_1x + A_2x^{5/3}$, where $A_0 = 0.53944$, $A_2 = -2.3$ are fitting parameters, and A_1 is held fixed by the measured system parameters with $\sigma = -0.107$. Dashed line is the same function but with A_2 set to zero, showing the asymptotic behavior at the approach to $T = 0$. The correlator $c(c\beta)^3\Delta B \approx 0.1686$ was computed numerically using Eq. (90) for the given aspect ratio, with ΔC and ΔD then given by Eq. (91) and Eq. (92) respectively.

tem, motivating a more detailed analysis of the finite-temperature depletion of n_s . As with the classical system, we will proceed by fitting our data not only with the theoretical T^3 -prediction, but also with a subleading correction proportional to T^5 . Simulating a reliable value of the parameter σ proves once again to be a non-trivial task. Here, instead of trying to extrapolate σ from simulations of small systems, we adopt a different approach: Since depletion of n_s in an isotropic system depends on the two parameters β and $\lambda_\beta = c\beta/L$ (see Sec. IIID), we choose to simulate two different systems, with different values of λ_β . That is to say, while varying temperature in the simulations, we also vary system size such that λ_β is fixed to the same value for all data points. By manually varying σ and the ground-state value $n_s(T = 0)$ (which should be the same for both systems), we can verify the theory by finding values of σ and $n_s(T = 0)$ that can predict the depletion in both cases.

Figure 9 shows n_s as a function of $(T/c)^3$ for $L \approx 4.698c\beta$, and Fig. 10 shows the same for $L = c\beta$. While the data in Fig. 9 could in principle be well described by the asymptotic formula (73), in the interest of maximal accuracy, we opt instead to compute Δn_s using the results of Sec. IIID. For $L \approx 4.698c\beta$ we find numerically $c(c\beta)^3\Delta B \approx 0.1686$, with Eqs. (91) and (92) yielding the remaining correlators. For the $L = c\beta$ case, the exact analytical result is given by Eq. (93). We find that both sets of data are fitted well when $\sigma = -0.107$. This is in slight contrast to the available data from the winding number estimator (97), shown in Fig. 11, which seems to indicate $\sigma \approx -0.15$. However, the significant statistical

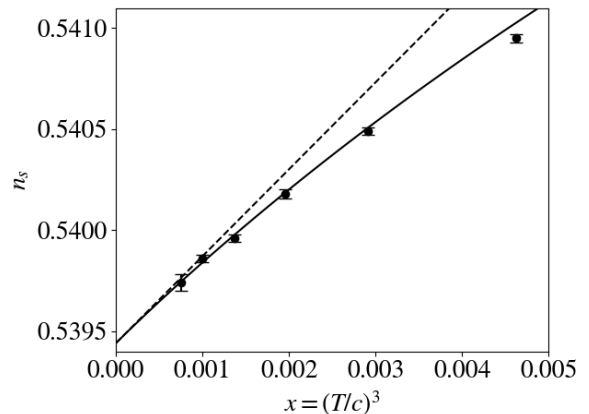


FIG. 10. The interplay of finite- β and finite-size effects on the superfluid stiffness in a square system of hard-core bosons at half-filling. System size is such that $c\beta = L$. As suggested by Eq. (93), the stiffness increases as the temperature increases because of the simultaneous decrease of the system size. Solid line is a fit of the form $A_0 + A_1x + A_2x^{5/3}$, where $x = (T/c)^3$, and A_1 is fixed by Eq. (93) with $\sigma = -0.107$. A_0 and A_2 are fitting parameters, with the fit yielding $A_0 = 0.53944$ and $A_2 = -3.15$. Dashed line is the same curve with A_2 set to zero, showing the low-temperature T^3 law predicted by the theory.

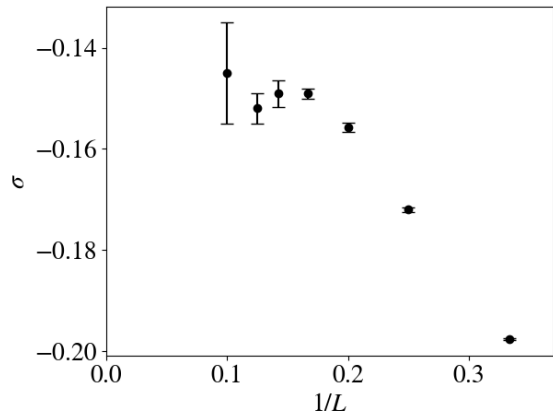


FIG. 11. Winding number estimator (97) for σ as a function of inverse system size. Temperature is chosen such that $c\beta = L$ for each data point. There is an apparent plateau at $\sigma \approx -0.15$. However, the strong finite-size effects and large statistical uncertainties prevent a reliable $L \rightarrow \infty$ extrapolation.

errors in the winding number data makes it hard to extrapolate a reliable value for σ , as it is not certain if the trend changes at larger system sizes or not. In principle it is also possible to extract σ from Eq. (84), similarly to what was done for the classical system. It turns out not to be as practical for the quantum system however, due to significant finite-size effects preventing any reliable extrapolation from the few accessible data points.

V. CONCLUSION

We developed a field-theoretical framework for calculating finite-size corrections to harmonic terms of a $U(1)$ -symmetric effective action. The corrections are due to truncation of the renormalization of the harmonic terms by the non-harmonic ones. We applied our theory to the problem of the low-temperature depletion of superfluid stiffness in a generic superfluid. The depletion is controlled by the three parameters: ν , γ , and σ , with the result expressed by Eqs. (2)–(4). In a Galilean system, parameters γ and σ are identically equal to zero and ν equals to the inverse particle mass. This is how Eqs. (2)–(4) recover Landau’s relation, while simultaneously revealing its deficiency in a generic case.

At the qualitative level, our analysis predicts phenomena fundamentally absent from the Landau theory. While a Galilean system will have a ground-state superfluid density exactly equal to the total density at all system sizes, in the general case, one will see finite-size corrections described by Eqs. (82) and (83). The form of Eq. (2) also suggests that there might exist exotic regimes where one can see *enhancement* of the superfluid density instead of depletion.

It is important to realize that even at $\gamma = \sigma = 0$, the requirement $\nu = 1/m$ is *necessary* for the depletion of the superfluid density $-\Delta\rho_s = -m\Delta n_s$ to coincide with the “normal density” of the phonon wind, n_{wind} . Based on the definition (with v_0 the velocity of the wind)

$$n_{\text{wind}} = \lim_{v_0 \rightarrow 0} |\langle \mathbf{j} \rangle| / v_0, \quad (103)$$

we readily calculate n_{wind} from the harmonic part of the hydrodynamic Hamiltonian. The leading contribution comes from the second term in the r.h.s. of (43) yielding the relation between $-\Delta\rho_s$ and n_{wind} :

$$-\Delta\rho_s = \nu m n_{\text{wind}} \quad (\gamma = \sigma = 0). \quad (104)$$

This way we prove that in a general case, the phonon wind and thermal depletion of superfluid density are fundamentally different phenomena.

The fact that our theory reproduces the result of Landau should be considered as an important and nontrivial check point. Further and more general validation is provided by numeric simulations. The agreement with numeric results is satisfactory but there is still room for further work. The main challenge is associated with direct estimation of parameter σ . Small system sizes are not sufficient because of large systematic error, while for linear system sizes larger than 10 the signal becomes smaller than statistical noise. It might also be useful to further

develop theory to understand the scaling of subleading corrections to the finite-temperature (finite-size) effects to be able to fit numeric data—clearly showing the importance of subleading terms—with corresponding ansatz.

Finally, we would like to comment on the broader context of the developed theory. Focusing on the problem of the thermal depletion of the superfluid density at constant density $\Delta n_s(n, T)$, we adjusted our formalism, grand canonical in its nature, to produce canonical results without developing full-scale universal low-temperature thermodynamics of a superfluid. If we took the latter approach straightforwardly working with Popov’s action, our result for $\Delta n_s(n, T)$ would come in the form

$$\Delta n_s(n, T) = \Delta n_s(\mu, T) - \nu \Delta n(\mu, T), \quad (105)$$

where $\Delta n_s(\mu, T)$ and $\Delta n(\mu, T)$ are thermal depletions of n_s and n at constant chemical potential. The second term in the r.h.s. is of a simple quasi-ground-state nature; it accounts for the change of the ground-state value of n_s due to the change in density. While both $\Delta n_s(\mu, T)$ and $\Delta n(\mu, T)$ depend on the cubic in η term in the hydrodynamic Hamiltonian/action, corresponding terms should cancel each other so that the term proves irrelevant for $\Delta n_s(n, T)$, as is clear from our results.

Having said that, it should also be emphasized that full-scale low-temperature universal thermodynamics of superfluids is of great interest on its own. Consider two superfluids consisting of the same type of superfluid matter (but not necessarily having the same microscopic structure—like, *e.g.*, uniform ^4He liquid and ^4He in this or that porous medium) are connected by a link suppressing the normal flow thus allowing for a temperature difference between the two samples sharing one and the same chemical potential. Within this textbook fountain-type setup [13], the two equations of states, $\Delta n_1(\mu, T_1)$ and $\Delta n_2(\mu, T_2)$, describe the redistribution of matter between the two superfluids as a response to two temperatures, T_1 and T_2 . Corresponding theory will be developed in a separate publication [17].

ACKNOWLEDGMENTS

This work was stimulated by numerous conversations (though without reaching a consensus [18]) with Wei Ku about the scientific status of Landau theory of low-temperature depletion of superfluid density.

This work was supported by the National Science Foundation under Grant DMR-2335904.

[1] L. Landau. Theory of the superfluidity of helium ii. *Phys. Rev.*, 60:356–358, Aug 1941.

[2] P. W. Anderson. Considerations on the flow of superfluid helium. *Rev. Mod. Phys.*, 38:298–310, Apr 1966.

- [3] L. Onsager. Statistical hydrodynamics. *Il Nuovo Cimento (1943-1954)*, 6(2):279–287, Mar 1949.
- [4] R.P. Feynman. Chapter ii application of quantum mechanics to liquid helium. volume 1 of *Progress in Low Temperature Physics*, pages 17–53. Elsevier, 1955.
- [5] E. L. Andronikashvili and Yu. G. Mamaladze. Quantization of macroscopic motions and hydrodynamics of rotating helium ii. *Rev. Mod. Phys.*, 38:567–625, Oct 1966.
- [6] B.D. Josephson. Possible new effects in superconductive tunnelling. *Physics Letters*, 1(7):251–253, 1962.
- [7] J. B. Mehl and W. Zimmermann. Flow of superfluid helium in a porous medium. *Phys. Rev.*, 167:214–229, Mar 1968.
- [8] M. Boninsegni. Thin helium film on a glass substrate. *Journal of Low Temperature Physics*, 159(3):441–451, May 2010.
- [9] I.M. Khalatnikov. *An Introduction To The Theory Of Superfluidity*. CRC Press, 2018.
- [10] Nikolay V. Prokof’ev and Boris V. Svistunov. Two definitions of superfluid density. *Phys. Rev. B*, 61:11282–11284, May 2000.
- [11] E. L. Pollock and D. M. Ceperley. Path-integral computation of superfluid densities. *Phys. Rev. B*, 36:8343–8352, Dec 1987.
- [12] Nikolay Prokof’ev and Boris Svistunov. Worm algorithms for classical statistical models. *Phys. Rev. Lett.*, 87:160601, Sep 2001.
- [13] B. Svistunov, E. Babaev, and N. Prokof’ev. *Superfluid States of Matter*. Taylor & Francis, 2015.
- [14] V.N. Popov. *Functional Integrals in Quantum Field Theory and Statistical Physics*. Springer Dordrecht, 1983.
- [15] N. V. Prokof’ev, B. V. Svistunov, and I. S. Tupitsyn. Exact, complete, and universal continuous-time worldline monte carlo approach to the statistics of discrete quantum systems. *Journal of Experimental and Theoretical Physics*, 87(2):310–321, Aug 1998.
- [16] M. Boninsegni, N. V. Prokof’ev, and B. V. Svistunov. Worm algorithm and diagrammatic monte carlo: A new approach to continuous-space path integral monte carlo simulations. *Phys. Rev. E*, 74:036701, Sep 2006.
- [17] Viktor Berger, Nikolay Prokof’ev, and Boris Svistunov. *Work in progress*.
- [18] Anthony Hegg, Ruoshi Jiang, Jie Wang, Jinning Hou, Tao Zeng, Yucel Yildirim, and Wei Ku. Universal low-temperature fluctuation of unconventional superconductors revealed: “smoking gun” leaves proper bosonic superfluidity the last theory standing. *arXiv:2402.08730 [cond-mat.supr-con]*, 2024.

Appendix A: Useful mathematical relations

Each expression for regularized correlators of interest can be reduced to the evaluation of some dimensionless constant, α , given by a d -dimensional integral over \mathbf{q} with an integrand being a regularized sum, $\Sigma(q)$, times q raised to a certain integer power l :

$$\alpha = \int \frac{d^d q}{(2\pi)^d} q^l \Sigma(q), \quad (\text{A1})$$

$$\Sigma(q) = \lim_{n_* \rightarrow \infty} \left[\sum_{n=-n_*}^{n_*} f(q, n) - \int_{n=-n_*}^{n_*} f(q, n) dn \right]. \quad (\text{A2})$$

As described above, the regularization of the sum amounts to subtracting the corresponding integral. If the sum and integral converge, then n_* can be replaced with ∞ in the sum and integral individually.

The first case of this type is

$$\alpha_1 = \int \frac{d^d q}{(2\pi)^d} q^2 \Sigma_1(q), \quad (\text{A3})$$

$$f_1(q, n) = \frac{1}{(2\pi n)^2 + q^2}. \quad (\text{A4})$$

Using standard mathematical result

$$\sum_{n=-\infty}^{\infty} \frac{1}{(2\pi n)^2 + q^2} = \frac{1}{2q} \coth(q/2), \quad (\text{A5})$$

we arrive at

$$\alpha_1 = \int \frac{d^d q}{(2\pi)^d} \frac{q}{e^q - 1} = I_d. \quad (\text{A6})$$

The second case is

$$\alpha_2 = \int \frac{d^d q}{(2\pi)^d} q^4 \Sigma_2(q), \quad (\text{A7})$$

$$f_2(q, n) = \frac{1}{[(2\pi n)^2 + q^2]^2}. \quad (\text{A8})$$

Here we observed that

$$\Sigma_2(q) = -\frac{1}{2q} \frac{d\Sigma_1(q)}{dq},$$

which allows us to relate α_2 to α_1 by doing the integral in (A7) by parts:

$$\alpha_2 = \frac{d+2}{2} \alpha_1 = \frac{d+2}{2} I_d. \quad (\text{A9})$$

At the first glance, the third case

$$\alpha_3 = \int \frac{d^d q}{(2\pi)^d} q^2 \Sigma_3(q), \quad (\text{A10})$$

$$f_3(q, n) = \frac{(2\pi n)^2}{[(2\pi n)^2 + q^2]^2}, \quad (\text{A11})$$

requires careful regularization. However, by observing that

$$f_3(q, n) = \frac{1}{(2\pi n)^2 + q^2} - \frac{q^2}{[(2\pi n)^2 + q^2]^2},$$

we immediately conclude that

$$\alpha_3 = \alpha_1 - \alpha_2 = -\frac{d}{2} I_d. \quad (\text{A12})$$

The fourth case

$$\alpha_4 = \int \frac{d^d q}{(2\pi)^d} \Sigma_4(q), \quad (\text{A13})$$

$$f_4(q, n) = \frac{(2\pi n)^2}{(2\pi n)^2 + q^2}, \quad (\text{A14})$$

is processed similarly. Here we observe that

$$f_4(q, n) = 1 - \frac{q^2}{(2\pi n)^2 + q^2}.$$

The first term in the r.h.s. is n -independent and thus can be omitted because of exact cancellation between the sum and the regularizing integral. We conclude that

$$\alpha_4 = -\alpha_1 = -I_d. \quad (\text{A15})$$

Appendix B: Symmetrization of integrals

The substitution $x_i^2 \rightarrow r^2/d$ in an integral, where $r^2 = \sum_i x_i^2$, is trivial given that the expression multiplying x_i^2 in the integrand is an isotropic function. This relation can be generalized to higher order (in x_i) polynomials as follows:

Let $\mathbf{r} = (x_1, \dots, x_d)$ be a d -dimensional vector and $f(r)$ some function that depends only on the magnitude r of the vector \mathbf{r} . Consider an integral

$$I = \int d^d r \left(\prod_{j=1}^d x_j^{2\alpha_j} \right) f(r), \quad (\text{B1})$$

where α_j 's are certain nonnegative integers. Integrating first over the surface of the hypersphere of the hyperradius r ,

$$\int_{S_r} dS \prod_{j=1}^d x_j^{2\alpha_j}$$

and observing that [below $S(r)$ is the hyper-area of the hypersphere \mathcal{S}_r]

$$\Theta = \frac{1}{S(r) r^{2\alpha_*}} \int_{\mathcal{S}_r} dS \prod_{j=1}^d x_j^{2\alpha_j} \quad \left(\alpha_* = \sum_{j=1}^d \alpha_j \right)$$

is an r -independent function of $\vec{\alpha} = (\alpha_1, \dots, \alpha_d)$, we conclude that the integral (B1) reduces to the following isotropic form

$$I = \Theta(\vec{\alpha}) \int r^{2\alpha_*} f(r) d^d r. \quad (\text{B2})$$

The function $\Theta(\vec{\alpha})$ is readily found by explicitly calculating the integral I_0 corresponding to $f(r) = e^{-r^2}$. On the

one hand, using the original form (B1), we have

$$I_0 = (-1)^{\alpha_*} \left(\prod_{\substack{j=1 \\ \alpha_j \neq 0}}^d \frac{\partial^{\alpha_j}}{\partial \lambda_j^{\alpha_j}} \right) \int d^d r \exp \left(- \sum_{j=1}^d \lambda_j x_j^2 \right) \Big|_{\lambda_j=1}.$$

On the other hand, from the representation (B2) we are supposed to have

$$I_0 = \Theta(\vec{\alpha}) (-1)^{\alpha_*} \frac{d^{\alpha_*}}{d\lambda^{\alpha_*}} \int d^d r \exp \left(-\lambda \sum_{j=1}^d x_j^2 \right) \Big|_{\lambda=1}.$$

Now explicitly performing the Gaussian integrals in both expressions and then requiring that the two results for I_0 be equal, we find

$$\Theta(\vec{\alpha}) = \left(\frac{d^{\alpha_*} \lambda^{-d/2}}{d\lambda^{\alpha_*}} \Big|_{\lambda=1} \right)^{-1} \prod_{\substack{j=1 \\ \alpha_j \neq 0}}^d \left(\frac{d^{\alpha_j} \lambda^{-1/2}}{d\lambda^{\alpha_j}} \Big|_{\lambda=1} \right). \quad (\text{B3})$$